

# Single Spin Asymmetries in Heavy Quark and Antiquark Productions

Feng Yuan\*

*Nuclear Science Division, Lawrence Berkeley National Laboratory, Berkeley, CA 94720 and  
RIKEN BNL Research Center, Building 510A,  
Brookhaven National Laboratory, Upton, NY 11973*

Jian Zhou†

*Nuclear Science Division, Lawrence Berkeley National Laboratory, Berkeley, CA 94720 and  
Department of Physics, Shandong University, Jinan, Shandong 250100, China*

## Abstract

The single transverse spin asymmetries in heavy quark and anti-quark production from the quark-antiquark annihilation channel contribution is studied by taking into account the initial and final state interactions effects. Because of the different color charges, the final state interaction effects lead to about a factor of 3 difference in the spin asymmetry for heavy quark over that for the anti-quark in the valence region of low energy  $pp$  collisions. The experimental study of this model-independent prediction shall provide a crucial test for the underlying mechanism for the single spin asymmetry phenomena.

---

\*Electronic address: [fyuan@lbl.gov](mailto:fyuan@lbl.gov)

†Electronic address: [jzhou@lbl.gov](mailto:jzhou@lbl.gov)

**1. Introduction.** Single-transverse spin asymmetry (SSA) is a novel and long standing phenomena in hadronic reactions [1, 2], and has attracted intensive interests from both experiment and theory sides in the last few years. It is a transverse spin dependent observable, defined as the ratio of the cross section difference when we flip the transverse spin of one of the hadrons involved in the scattering over the sum of the cross sections,  $A_N \propto (d\sigma(S_\perp) - d\sigma(-S_\perp))/(d\sigma(S_\perp) + d\sigma(-S_\perp))$ . The experimental observation of SSAs in semi-inclusive hadron production in deep inelastic scattering (SIDIS), in inclusive hadron production in  $pp$  scattering at collider energy at RHIC, and the relevant azimuthal asymmetric distribution of hadron production in  $e^+e^-$  annihilation have motivated the theoretical developments in the last few years. It was also argued that the SSA phenomena is closely related to the orbital motion of quarks and gluons in the nucleon [3–5].

Theoretically, it has been realized that the initial/final state interactions are crucial to leading to a nonzero SSA in high energy scattering [2, 3]. These effects also invalidate the naive-time-reversal invariance argument [6–9] for the non-existence of the so-called Sivers function [10], which describes a correlation between the intrinsic transverse momentum of parton and the transverse polarization vector of the nucleon. The initial/final state interaction effects introduce a process-dependence in the SSA observables. For example, the SSA in the SIDIS process comes from final state interaction whereas that in the Drell-Yan lepton pair production comes from the initial state interaction. The consequence of this difference is that there is a sign change between the SSAs for these two processes [7, 11]. It is of crucial to test this nontrivial QCD predictions by comparing the SSAs in these two processes. The Sivers single spin asymmetry in SIDIS process has been observed by the HERMES collaboration [12], and the planned Drell-Yan measurement at RHIC and other facility will test this prediction [13].

In this paper, we study another interesting probe for the initial/final state interaction effects: the SSAs in heavy quark and antiquark production in hadronic process. Because the heavy quark and antiquark can be detected by their decay products, their SSAs can be measured separately. The heavy quark and antiquark produced in short distance partonic processes will experience different final state interactions with the nucleon remanet due to their different color charges, and therefore the SSAs for heavy quark and antiquark will be different. Detailed calculations in the following show that the difference could be as large as a factor of 3 if the quark-antiquark channel contribution dominates. This is a direct

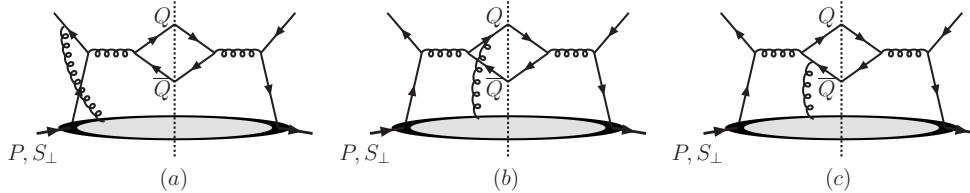


FIG. 1: *Initial/final state interactions contributions to the SSAs in heavy quark and antiquark productions: (a) initial state interaction with color strength  $1/2N_c$ ; (b) final state interaction on the quark line with color strength  $(N_c^2 - 2)/2N_c$ ; (c) final state interaction on the antiquark line with color strength  $2/2N_c$ . The mirror diagrams where the gluon attaches to the right of the cut line are not shown, but also contribute.*

consequence of the final state interaction effects in these SSAs.

The rest of the paper is organized as follows. In Sec.2, we will set up our framework, and calculate the SSAs for heavy quark and antiquark in the twist-three quark-gluon correlation approach [2, 14] and the initial/final state interactions effects are properly taken into account. We further present some numerical results for experiments at low energy  $pp$  scattering where the quark-antiquark channel dominates, and we will observe a factor of 3 difference between heavy quark and antiquark SSAs. We conclude our paper in Sec. 3.

**2. SSAs in Heavy Quark and Antiquark Productions.** In order to obtain a non-zero SSA in high energy process, we must generate a phase from parton re-scattering in hard process [2, 3]. Similar to other hadronic processes, in the heavy quark production in  $pp$  collisions [2, 14], the partons involved in the re-scattering can come from the initial state or final state, and they are referred as the initial and final state interactions, respectively. Because of the different color charges they carried in the scattering process, the heavy quark and antiquark will have different effects from the final state interactions. The initial state interactions, on the other hand, are the same for both particles. In this paper, we will take the quark-antiquark annihilation channel as an example to demonstrate the unique consequence from the different final state interaction effects on the heavy quark and antiquark productions. The light quark production in this channel has been studied in [2, 14]. We will extend to the heavy quark production and study the relevant phenomenological consequence.

In the quark-antiquark annihilation channel, the quark (or antiquark) from the polarized nucleon annihilates the antiquark (or quark) from the unpolarized nucleon, and produces a

heavy quark and antiquark pair. For the spin-average cross section, this forms the  $s$ -channel partonic diagram. As we mentioned above, the single transverse spin dependent cross section comes from both initial and final state interaction contributions. In Fig. 1 we show the relevant initial (a) and final state interactions (b,c) diagrams. Different from those in the SIDIS and Drell-Yan lepton pair production, these initial and final state interactions have different strength because they have different color charges. This will result into different color-factors for them, which can be carried out in a model-independent way. For example, for the initial state interaction of Fig. 1(a), we can label the incoming quark legs from the polarized nucleon with color-index  $i$  and  $j$  ( $(i, j) = 1, 3$  in the elementary representation in the  $SU(3)$  gauge group), the additional gluon with index  $a$  ( $a = 1, 8$  for the adjoint representation) connecting the nucleon remanet with the partons in the hard partonic processes. The color-matrix representing the coupling of the nucleon with the partonic part will be uniquely the  $SU(3)$  color matrices  $T_{ij}^a$ , because of the gauge invariance. Therefore, the color-factor associated with the initial state interaction can be formulated as

$$\text{Fig.1(a)} \propto (-)\text{tr} [T^a T^b T^a T^c] \times \text{tr} [T^b T^c] = \frac{1}{2N_C} \frac{N_c^2 - 1}{4}, \quad (1)$$

where the additional minus sign is due to the initial state interaction effect. Similarly, the final state interaction diagram of Fig. 1(b) will be

$$\text{Fig.1(b)} \propto \text{tr} [T^a T^b T^c] \times \text{tr} [T^b T^a T^c] = \frac{N_C^2 - 2N_c^2 - 1}{2N_C} \frac{1}{4}. \quad (2)$$

Because this final state interaction is on the quark line, there is no additional minus sign. However, the final state interaction on the antiquark line will have a minus sign,

$$\text{Fig.1(c)} \propto (-)\text{tr} [T^a T^b T^c] \times \text{tr} [T^a T^b T^c] = \frac{2}{2N_C} \frac{N_c^2 - 1}{4}. \quad (3)$$

From the above results, we find that all the initial and final state interactions contribute the same sign. However, the strengths of these interactions are different. Especially, the two final state interactions differ by a factor of 3.

Furthermore, the initial state interaction diagram Fig. 1(a) contributes to the SSAs in both heavy quark and antiquark productions. However, the final state interaction on the quark line Fig. 1(b) only contributes to the heavy quark SSA, whereas that on the antiquark line Fig. 1(c) only contributes to that for the antiquark. For example, when we study the SSA for heavy quark production, the kinematics of heavy antiquark is integrated out. The

phase contribution from the final state interaction on the antiquark line (Fig. 1(c)) will cancel out that from the same diagram but with the gluon attachment to the right of the cut line (the mirror diagram of Fig. 1(c)) [2]. Therefore, the heavy quark SSA has contribution from the initial state interaction of Fig. 1(a) and the final state interaction on the quark line Fig. 1(b), whereas the heavy antiquark SSA from the initial state interaction of Fig. 1(a) and the final state interaction on the antiquark line Fig. 1(c). If the final state interactions dominate their SSAs, we will expect a factor of 3 difference between the SSAs in heavy quark and antiquark productions, because of the different strengths they have as we have shown in the above analysis. This is a model independent observation. Its test shall provide a strong support for the underlying physics for the SSA phenomena.

To calculate the SSA contributions from these diagrams, it is appropriate to adopt the twist-three quark-gluon-antiquark correlation approach developed in [2], because the heavy quark mass provides a natural hard scale in the computation of the perturbative diagrams, and the collinear factorization approach is applicable. An important feature from this approach is that the single spin asymmetry is naturally suppressed in the limit of  $P_\perp \ll M_Q$ , where  $P_\perp$  and  $M_Q$  are transverse momentum and mass of the heavy quark.

The calculations are similar to those in [2, 14], where the inclusive  $\pi$  production in  $p^\uparrow p \rightarrow \pi X$  was formulated. The only difference is that we have to restore the mass dependence for the final state quark and antiquark. The spin-average cross section can be summarized as,

$$E_Q \frac{d^3\sigma}{d^3P_Q} = \frac{\alpha_s^2}{S} \int \frac{dx'}{x'} f_b(x') \frac{f_a(x)}{x} \frac{1}{x'S + (T - M_Q^2)} H_{ab \rightarrow Q\bar{Q}}^U(\tilde{s}, \tilde{t}, \tilde{u}), \quad (4)$$

where  $P_Q$  is the heavy quark momentum,  $S$  the hadronic center of mass energy,  $S = (P_A + P_B)^2$  with  $P_A$  and  $P_B$  the momenta for the incident polarized and unpolarized nucleons,  $x$  and  $x'$  are the momentum fractions carried by the incident partons, and  $f_a$  and  $f_b$  are the associated parton distributions. The kinematic variables are defined as:  $E_Q = M_T \cosh y$  where  $M_T = \sqrt{M_Q^2 + P_\perp^2}$  and  $y$  is the rapidity for the heavy quark in the center of mass frame;  $T = M_Q^2 - M_T \sqrt{S} e^{-y}$  and  $U = M_Q^2 - M_T \sqrt{S} e^y$ ; the partonic variable  $\tilde{s} = xx'S$ ,  $\tilde{t} = -xM_T \sqrt{S} e^{-y}$ , and  $\tilde{u} = -x'M_T \sqrt{S} e^y$ . The leading contribution to heavy quark production comes from quark-antiquark and gluon-gluon channels, and their hard factor  $H^U$  are defined

as,

$$H_{q\bar{q}\rightarrow Q\bar{Q}}^U = \frac{N_c^2 - 1}{4N_c^2} \frac{2(\tilde{t}^2 + \tilde{u}^2 + 2M_Q^2\tilde{s})}{\tilde{s}^2}, \quad (5)$$

$$H_{g\bar{g}\rightarrow Q\bar{Q}}^U = \frac{2}{4N_c} \left( \frac{1}{\tilde{t}\tilde{u}} - \frac{2N_c^2}{N_c^2 - 1} \frac{1}{\tilde{s}^2} \right) \frac{\tilde{t}\tilde{u}(\tilde{t}^2 + \tilde{u}^2 + 4\tilde{M}_Q^2) - 4\tilde{s}^2 M_Q^4}{\tilde{t}\tilde{u}}. \quad (6)$$

In the twist-three framework [2], the single transverse spin dependent cross section depends on the twist-three quark-gluon correlation function, the so-called Qiu-Sterman matrix element. They are defined as

$$T_F^q(x_1, x_2) \equiv \int \frac{d\zeta^- d\eta^-}{4\pi} e^{i(k_{q1}^+ \eta^- + k_g^+ \zeta^-)} \epsilon_{\perp}^{\beta\alpha} S_{\perp\beta} \quad (7)$$

$$\langle PS | \bar{\psi}_q(0) \mathcal{L}(0, \zeta^-) \gamma^+ g F^+_{\alpha}(\zeta^-) \mathcal{L}(\zeta^-, \eta^-) \psi_q(\eta^-) | PS \rangle,$$

where the sums over color and spin indices are implicit,  $\epsilon^{\beta\alpha} \equiv \epsilon^{\mu\nu\beta\alpha} P_{A\mu} P_{B\nu} / P_A \cdot P_B$  with  $\epsilon^{0123} = 1$ ,  $|PS\rangle$  denotes the proton state,  $\psi$  the quark field,  $F^+_{\alpha}$  the gluon field tensor, and  $\mathcal{L}$  represents the gauge link to make the above definition gauge invariant. By summing the initial and final state interaction contributions, the single spin dependent differential cross section for heavy quark production can be written as

$$E_Q \frac{d^3 \Delta\sigma(S_{\perp})}{d^3 P_Q} = \frac{\alpha_s^2}{S} \int \frac{dx'}{x'} f_{\bar{q}}(x') \frac{\epsilon^{\alpha\beta} S_{\perp}^{\alpha} P_{\perp}^{\beta}}{x' S + (T - M_Q^2) \tilde{u}} \frac{1}{\tilde{u}} \left\{ \left( \frac{T_F^q(x)}{x} - \frac{\partial}{\partial x} T_F^q(x) \right) \right.$$

$$\left. \times H_{q\bar{q}\rightarrow Q} + \frac{T_F^q(x)}{x} \tilde{H}_{q\bar{q}\rightarrow Q} \right\}, \quad (8)$$

where  $T_F^q(x) \equiv T_F^q(x, x)$ . A similar expression can be obtained for the antiquark by replacing  $Q \rightarrow \bar{Q}$  in the above. The above hard factors include both initial and final state interaction contributions. The first term  $H_{q\bar{q}\rightarrow Q}$  follows a compact formula containing the derivative and non-derivative (of the twist-three function) contributions [14], whereas the second term  $\tilde{H}_{q\bar{q}\rightarrow Q}$  only depends on the non-derivative of the twist-three correlation function and vanishes in the massless limit  $M_Q \rightarrow 0$ . Under this limit, our results reproduce the relevant formula in [14]. The hard factors are found,

$$H_{q\bar{q}\rightarrow Q} = H_{q\bar{q}\rightarrow Q}^I + H_{q\bar{q}\rightarrow Q}^F \left( 1 + \frac{\tilde{u}}{\tilde{t}} \right), \quad (9)$$

$$\tilde{H}_{q\bar{q}\rightarrow Q} = \tilde{H}_{q\bar{q}\rightarrow Q}^I + \tilde{H}_{q\bar{q}\rightarrow Q}^F \left( 1 + \frac{\tilde{u}}{\tilde{t}} \right), \quad (10)$$

where

$$H_{q\bar{q}\rightarrow Q}^I = H_{q\bar{q}\rightarrow \bar{Q}}^I = \frac{1}{4N_c^2} \frac{2(\tilde{t}^2 + \tilde{u}^2 + 2M_Q^2\tilde{s})}{\tilde{s}^2}, \quad \tilde{H}_{q\bar{q}\rightarrow Q}^I = \tilde{H}_{q\bar{q}\rightarrow \bar{Q}}^I = \frac{1}{N_c^2} \frac{M_Q^2}{\tilde{s}}, \quad (11)$$

$$H_{q\bar{q}\rightarrow Q}^F = \frac{N_c^2 - 2}{4N_c^2} \frac{2(\tilde{t}^2 + \tilde{u}^2 + 2M_Q^2\tilde{s})}{\tilde{s}^2}, \quad \tilde{H}_{q\bar{q}\rightarrow Q}^F = \frac{N_c^2 - 2}{N_c^2} \frac{M_Q^2}{\tilde{s}}, \quad (12)$$

$$H_{q\bar{q}\rightarrow \bar{Q}}^F = \frac{2}{4N_c^2} \frac{2(\tilde{t}^2 + \tilde{u}^2 + 2M_Q^2\tilde{s})}{\tilde{s}^2}, \quad \tilde{H}_{q\bar{q}\rightarrow \bar{Q}}^F = \frac{2}{N_c^2} \frac{M_Q^2}{\tilde{s}}, \quad (13)$$

where the color factors have been discussed in the above. The contributions from the antiquark-gluon correlation functions can be obtained accordingly, by using the charge conjugation transformation.

It is important to note that the spin-average and spin-dependent cross section contributions are both well defined in the limit of  $P_\perp \rightarrow 0$ , because of the heavy quark mass. Therefore, the spin asymmetry defined as the ratio of these two cross section terms vanishes when  $P_\perp = 0$ . This is very different from the massless particle production where the single spin asymmetry divergent as  $1/P_\perp$  as  $P_\perp \rightarrow 0$  [2, 14]. Thus we can integrate out the cross sections to small transverse momentum region to obtain the spin asymmetry. In the following, we will present the numerical results for the conventional left-right asymmetry for the heavy quark production at low energy  $pp$  scattering. This asymmetry is defined as

$$A_N = \frac{L - R}{L + R}, \quad (14)$$

which counts the number difference between the left hand side and right hand side for heavy quark production from the moving direction of the polarized (upward) nucleon. It can be calculated from the cross section terms from above,

$$A_N = \frac{-\int_0^\pi d\phi d\Delta\sigma}{\int_0^\pi d\phi d\sigma}, \quad (15)$$

where  $\phi$  is the azimuthal angle of heavy quark transverse momentum  $P_\perp$  relative to the incoming nucleon transverse polarization vector  $S_\perp$ . In the following, we will show the above asymmetry for heavy quark and antiquark at low energy  $pp$  scattering where the quark-antiquark channel dominates. For the purpose of the demonstration, we adopt the parameterizations for the twist-three Qiu-Sterman matrix elements in the valence region as [14],

$$T_F^a(x) = N_a x^{\alpha_a} (1-x)^{\beta_a} q_a(x), \quad (16)$$

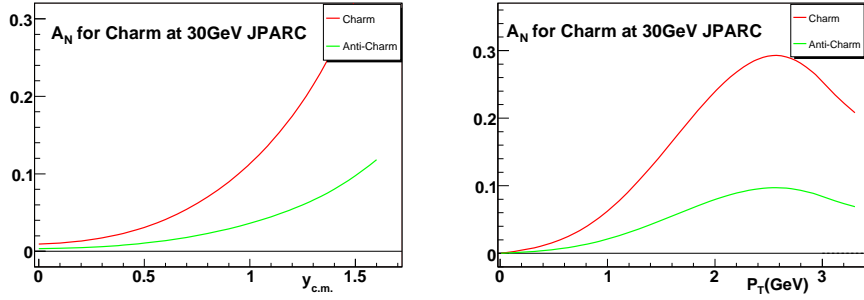


FIG. 2: Single spin asymmetries for charm quark and anticharm quark production in  $p^\uparrow p$  scattering at JPARC energy: as functions of rapidities with  $P_\perp$  integrated out (left panel); and as functions of transverse momentum  $P_\perp$  with  $y_{c.m.} > 0$  (right panel).

where  $q_a(x)$  is the unpolarized quark distribution for flavor  $a$ . The above parameters for the valence  $u$  and  $d$  quarks were determined from a comparison to the single spin asymmetry data in  $p^\uparrow p \rightarrow \pi X$  [14], and they are also compatible with the SIDIS data from HERMES [15]. For the unpolarized parton distributions, we use the leading order (LO) CTEQ5L parton distribution functions [16].

In Fig. 2, we show our predictions for the heavy quark and antiquark single spin asymmetries in  $p^\uparrow p$  scattering at JPARC energy region ( $\sqrt{s} \approx 7.8\text{GeV}$ ), where we expect the quark-antiquark annihilation channel dominates the cross section. The left panel shows the asymmetries  $A_N$  as functions of the center of mass rapidities of the charm quark and anti-charm quark with the transverse momentum  $P_\perp$  integrated out; the right panel shows the asymmetries as functions of the transverse momentum  $P_\perp$  in the forward rapidity region ( $y_{c.m.} > 0$ ). From these plots, we find that the asymmetries increase with rapidity, similar to the general trend in other SSA observations [14]. More importantly, the single spin asymmetry for the charm quark is much larger than that for anticharm quark in the full rapidity range. Similar observation was found for the asymmetries as functions of the transverse momentum  $P_\perp$ . Both asymmetries vanish as  $P_\perp \rightarrow 0$  as we expected.

In Fig. 3, we show the predictions at  $\sqrt{s} = 14\text{GeV}$   $p^\uparrow \bar{p}$  scattering at the PAX experiment at GSI PAIR. Because the quark-antiquark channel always dominates the cross section, we find a sizable SSA for charm quark even at central rapidity region. Again, we observe that the SSA for charm quark is about a factor of 3 larger than that for the anticharm quark. In this experiment, we can further study the spin asymmetry with the antiproton transversely

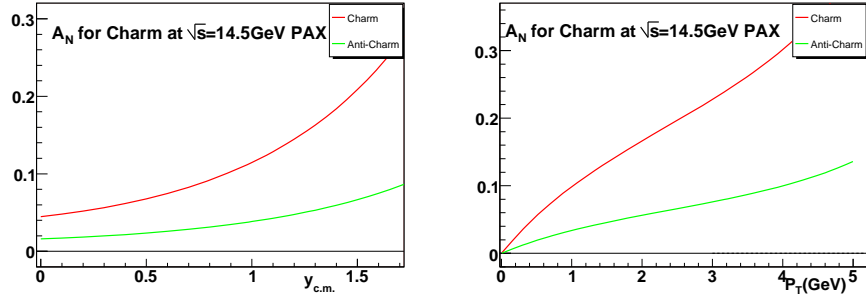


FIG. 3: *Single spin asymmetries for charm and anticharm quark production in  $p^\uparrow\bar{p}$  scattering at  $\sqrt{s} = 14\text{GeV}$  at PAX energy region: as functions of rapidities with  $P_\perp$  integrated out (left panel); as functions of charm quark transverse momentum  $P_\perp$  with  $y_{c.m.} > 0$  (right panel).*

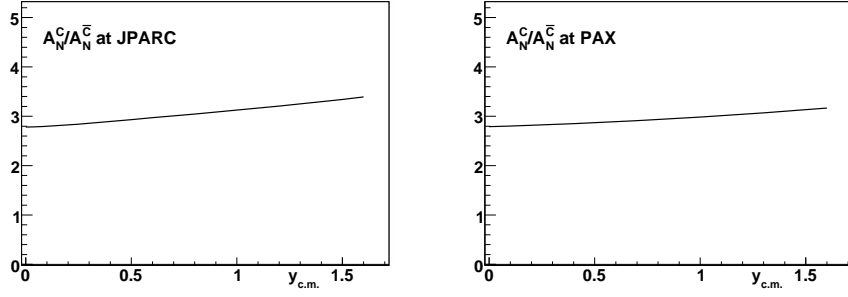


FIG. 4: *Ratio of the SSA for the charm quark over that for the anticharm quark as function of charm quark rapidity in  $p^\uparrow p$  scattering at JPARC (left) and  $\bar{p}^\uparrow p$  scattering at PAX (right) experiments.*

polarized  $\bar{p}^\uparrow p \rightarrow Q(\bar{Q})X$ , where we expect the SSA for anticharm quark is larger than that for the charm quark in the forward direction of the polarized antiproton. By using the charge conjugation transformation invariance, we will have the following relation between the SSAs in these two processes,

$$A_N(p^\uparrow\bar{p} \rightarrow C) = A_N(\bar{p}^\uparrow p \rightarrow \bar{C}) , \quad A_N(p^\uparrow\bar{p} \rightarrow \bar{C}) = A_N(\bar{p}^\uparrow p \rightarrow C) , \quad (17)$$

for the same kinematics. From these relations, we can obtain the corresponding results for  $\bar{p}^\uparrow p$  experiments from the plots in Fig. 3.

The sizes of the above single spin asymmetries also depend on the dominance of the quark-antiquark annihilation channel at both energies. In our leading order simulation with the CTEQ5L parameterization for the parton distributions, this channel indeed dominates the cross sections. These asymmetries may scale down if the gluon-gluon channel turns

dominant [17]. However, we shall still observe the big difference between the SSAs for charm and anticharm quarks when the twist-three gluon-gluon correlation contribution to the SSAs [18, 19] is small in the valence region. In order to demonstrate this difference, we plot in Fig. 4 the ratios of the asymmetries as functions of the rapidities at both experiments. From these plots, we find that the ratio at both experiments is about a factor of 3 and has little dependence on the rapidity. These ratios are model-independent predictions, especially at forward region of the polarized nucleon where the quark-antiquark channel dominates. We hope the experiments at both facilities can carry out these measurements, and test the predictions. We further notice that the sea quark contribution in the quark-gluon correlation functions from the polarized nucleon will be important at the central rapidities [14], where the above ratios may vary if we take into account those contributions.

**4. Summary.** In this paper, we studied the single spin asymmetries in heavy quark and antiquark production in hadronic processes. Because of the different color charges, the final state interactions on the heavy quark and antiquark are different, and therefore the associated single spin asymmetries are different too. Our numerical simulations showed that the single spin asymmetry for heavy quark is about a factor of 3 larger than that for the antiquark in the forward  $p^\uparrow p$  and  $p^\uparrow \bar{p}$  scattering at low energy scattering where the quark-antiquark channel dominates. The experimental observation of this unique signature shall provide a crucial test for the underlying physics for the single spin asymmetry phenomena.

In the above analysis, we only considered the quark-antiquark channel contributions. An extension to the gluon-channel contribution can follow accordingly, which will be relevant for the collider experiment at RHIC [18–20]. We reserve the study of this contribution as well as other contribution, for example, from the chiral-odd quark-gluon correlation functions [21] in a future publication. We further notice that the latter contribution will have the similar pattern for the SSAs in heavy quark and antiquark production as the chiral-even one as we discussed in this paper, because of the final state interaction effects dominate both contributions.

This work was supported in part by the U.S. Department of Energy under contract DE-AC02-05CH11231. We are grateful to RIKEN, Brookhaven National Laboratory and the U.S. Department of Energy (contract number DE-AC02-98CH10886) for providing the facilities essential for the completion of this work. J.Z. is partially supported by China Scholarship Council and National Natural Science Foundation of China under Project No.

- 
- [1] M. Anselmino, A. Efremov and E. Leader, Phys. Rept. **261**, 1 (1995) [Erratum-ibid. **281**, 399 (1997)]; Z. t. Liang and C. Boros, Int. J. Mod. Phys. A **15**, 927 (2000); V. Barone, A. Drago and P. G. Ratcliffe, Phys. Rept. **359**, 1 (2002).
- [2] J. w. Qiu and G. Sterman, Phys. Rev. Lett. **67**, 2264 (1991); Nucl. Phys. B **378**, 52 (1992); Phys. Rev. D **59**, 014004 (1999).
- [3] S. J. Brodsky, D. S. Hwang and I. Schmidt, Phys. Lett. B **530**, 99 (2002); Nucl. Phys. B **642**, 344 (2002).
- [4] X. Ji, J. P. Ma and F. Yuan, Nucl. Phys. B **652**, 383 (2003) [arXiv:hep-ph/0210430].
- [5] M. Burkardt, Phys. Rev. D **69**, 091501 (2004).
- [6] J. C. Collins, Nucl. Phys. B **396**, 161 (1993).
- [7] J. C. Collins, Phys. Lett. B **536**, 43 (2002).
- [8] X. Ji and F. Yuan, Phys. Lett. B **543**, 66 (2002); A. V. Belitsky, X. Ji and F. Yuan, Nucl. Phys. B **656**, 165 (2003).
- [9] D. Boer, P. J. Mulders and F. Pijlman, Nucl. Phys. B **667**, 201 (2003).
- [10] D. W. Sivers, Phys. Rev. D **43**, 261 (1991).
- [11] X. Ji, J. W. Qiu, W. Vogelsang and F. Yuan, Phys. Rev. Lett. **97**, 082002 (2006); Phys. Rev. D **73**, 094017 (2006); Phys. Lett. B **638**, 178 (2006).
- [12] A. Airapetian *et al.* [HERMES Collaboration], Phys. Rev. Lett. **84**, 4047 (2000); Phys. Rev. Lett. **94**, 012002 (2005).
- [13] Les Bland, *et al.*, RHIC proposal: “ *Transverse-Spin Drell-Yan Physics at RHIC*”, <http://spin.riken.bnl.gov/rsc/>.
- [14] C. Kouvaris, J. W. Qiu, W. Vogelsang and F. Yuan, Phys. Rev. D **74**, 114013 (2006) [arXiv:hep-ph/0609238].
- [15] F. Yuan, AIP Conf. Proc. **915**, 525 (2007).
- [16] H. L. Lai *et al.* [CTEQ Collaboration], Eur. Phys. J. C **12**, 375 (2000) [arXiv:hep-ph/9903282].
- [17] J. Riedl, A. Schafer and M. Stratmann, Eur. Phys. J. C **52**, 987 (2007) [arXiv:0708.3010 [hep-ph]].
- [18] X. D. Ji, Phys. Lett. B **289**, 137 (1992).

- [19] Z. B. Kang and J. W. Qiu, arXiv:0806.1970 [hep-ph].
- [20] M. Anselmino, M. Boglione, U. D'Alesio, E. Leader and F. Murgia, Phys. Rev. D **70**, 074025 (2004).
- [21] Y. Kanazawa and Y. Koike, Phys. Lett. B **478**, 121 (2000); Phys. Lett. B **490**, 99 (2000).